

Photoemission Insight into Heavy-Fermion Behavior in YbRh_2Si_2

D. V. Vyalikh,¹ S. Danzenbächer,¹ A. N. Yaresko,² M. Holder,¹ Yu. Kucherenko,^{1,3} C. Laubschat,¹ C. Krellner,⁴
Z. Hossain,^{4,5} C. Geibel,⁴ M. Shi,⁶ L. Patthey,⁶ and S. L. Molodtsov¹

¹*Institut für Festkörperphysik, Technische Universität Dresden, D-01062 Dresden, Germany*

²*Max-Planck-Institut für Physik Komplexer Systeme, Nöthnitzer Strasse 38, D-01187 Dresden, Germany*

³*Institute for Metal Physics, National Academy of Sciences of Ukraine, UA-03142 Kiev, Ukraine*

⁴*Max-Planck-Institut für Chemische Physik fester Stoffe, Nöthnitzer Strasse 40, D-01187 Dresden, Germany*

⁵*Department of Physics, Indian Institute of Technology, Kanpur-208016, India*

⁶*Swiss Light Source, Paul Scherrer Institute, CH-5232 Villigen-PSI, Switzerland*

(Received 19 July 2007; published 5 February 2008)

As shown by angle-resolved photoemission (PE), hybridization of bulk $\text{Yb } 4f^{2+}$ states with a shallow-lying valence band of the same symmetry leads in YbRh_2Si_2 to dispersion of a $4f$ PE signal in the region of the Kondo resonance with a Fermi-energy crossing close to $\bar{\Gamma}$. Additionally, renormalization of the valence state results in the formation of a heavy band that disperses parallel to the $4f$ originating signal. The symmetry and character of the states are probed by circular dichroism and the photon-energy dependence of the PE cross sections.

DOI: 10.1103/PhysRevLett.100.056402

PACS numbers: 71.20.Eh, 71.27.+a, 75.30.Mb, 79.60.-i

Heavy-fermion (HF) materials are known to reveal anomalous thermodynamic, transport and magnetic properties [1] that are caused by the formation of quasiparticle bands characterized by extremely large effective masses. Their values may lie in the range of 100 to 1000 free electron masses (m_0) as measured in magnetic susceptibility, specific heat, and resistivity experiments for CeCu_2Si_2 , CeNi_2Ge_2 , $\text{CeCu}_{6-x}\text{Au}_x$, and YbRh_2Si_2 [2]. Usually the thermodynamic and transport phenomena are analyzed applying the Kondo or Anderson Hamiltonian solved within the single-impurity Anderson model (SIAM) [3]. Unfortunately, SIAM ignores the translation symmetry of the lattice, and the mentioned low-energy excitation techniques provide results mostly averaged in reciprocal space. On the other hand, de Haas-van Alphen measurements give certain access to momentum (\mathbf{k}) dependent phenomena by probing mean values for a few extremal orbits associated with the Fermi surface [4]. However, the \mathbf{k} -dependent properties describing the dispersion of quasiparticle bands and, thus, the anisotropy of the heavy-fermion or Kondo behavior, remain largely unexplored.

Insight into the \mathbf{k} -dependent properties of single-crystalline HF systems can be achieved by angle-resolved photoemission (PE). Such PE studies are still rare owing to deficiency of superior equipment necessary to follow dispersions in extremely narrow-band materials. So far angle-resolved PE experiments were carried out for a number of single-crystalline heavy-fermion Ce and Yb samples. For Ce systems, predominantly intensity variations at the Fermi energy (E_F) were monitored [5,6]. In most studies [5], however, the analysis was performed applying SIAM that did not allow to achieve basic understanding of the observed \mathbf{k} -dependent phenomena.

Within a simplified approach to the periodic Anderson model (PAM) the corresponding intensity variations in

CePd_3 could be ascribed to changes of $4f$ hybridization related to the dispersive properties of valence bands (VBs) close to the Fermi energy [7]. Conclusions about dispersion of the Kondo resonance, however, are not straightforward, since the latter lies above E_F in Ce systems and only tails of the Kondo peak are accessible for PE. The effects of VB crossings on the dispersion of Ce $4f$ states could be studied for $4f$ emissions at higher binding energies (BEs): energy splittings of the $4f$ “ionization” peak (~ 2 eV BE) in a Ce monolayer on W(110) were observed that could be ascribed within PAM to the formation of symmetric and antisymmetric linear combinations of states [8].

Similar phenomena have been observed for Yb $4f$ emissions from YbIr_2Si_2 and YbRh_2Si_2 [9]. In these heavy-fermion compounds, hybridization with parabolic VBs leads to dispersion and energy splittings of the $4f^{13}$ surface signal around 0.6 eV BE that could be successfully modeled in the light of PAM. Since contrasting to Ce systems, the Kondo resonance lies below E_F in Yb-based HF compounds, there is additionally the unique possibility to study by PE bulk $\text{Yb } 4f^{2+}$ states in the immediate neighborhood of the Fermi energy, where respective interactions become relevant for thermodynamic and transport properties.

In the present contribution we report on an angle-resolved PE study of the electronic structure close to E_F in YbRh_2Si_2 [10]. We show that due to interaction with a VB the $4f$ states in the energy region of the Kondo resonance are pushed above E_F around the $\bar{\Gamma}$ point. A crossing with the band at higher \mathbf{k} values, as expected from band-structure calculations within the local-density approximation (LDA), is inhibited by the symmetry of the band that is the same as of the $4f$ state, as proved by circular dichroism in angular distribution of photoelectrons (CDAD) [11]. Instead, formation of a heavy electronic band with a dispersion parallel to the $4f$ originating signal is observed.

Single-crystalline samples [body-centered tetragonal ThCr_2Si_2 (space group $I4/mmm$) type] were grown from In flux in closed Ta crucible and characterized by x-ray diffraction, magnetic susceptibility, resistivity, and specific heat measurements. The measured Kondo temperature (T_K) amounts to ~ 25 K. Immediately before the PE measurements the samples (size $1 \times 1 \text{ mm}^2$) were cleaved *in situ* under ultrahigh vacuum conditions (10^{-11} Torr range). No sample aging was observed within the first 4 hours of data acquisition.

The experiments were performed at the Swiss Light Source (SLS, Surface and Interface: Spectroscopy beam line) using a Scienta 2002 analyzer. The spectra were taken at 55 eV and 110 eV photon energy in order to discriminate $4f$ and VB PE signals. While at $h\nu = 55$ eV both kind of states contribute to the PE intensity, at $h\nu = 110$ eV VB emission is weak. Particularly emission from Rh $4d$ states is suppressed due to a Cooper minimum of the PE cross section [12].

The experimental geometry is shown in Fig. 1. The analyzer was fixed, while the vertically mounted samples were rotated around the y axis. The incoming photon beam, the sample surface normal, and the analyzed PE directions were selected to be noncoplanar (except emission in the xz plane). In our experiments, either left (I_+) or right (I_-) circularly polarized radiation was used. Each time $\phi_{\pm} = 10^\circ$ photoemission cuts parallel to $\bar{\Gamma} - \bar{X}$ were covered. The samples were measured in the Kondo regime at $T \sim 20$ K. Momentum and energy resolutions were set to 0.011 \AA^{-1} or 0.016 \AA^{-1} and 15 meV or 30 meV for $h\nu = 55$ eV or $h\nu = 110$ eV, respectively.

Careful analysis of correlation effects requires as a first step identification of the VB spectral structures. Figure 2 presents a gray-scale PE plot measured in the Fermi-energy region close to the center of the surface Brillouin zone (BZ). In order to get rid of the CDAD effect, which interferes with the initial band assignment, the presented data exhibit the sum of PE intensities acquired with I_+ and I_- light polarizations. Two bands with holelike dispersion

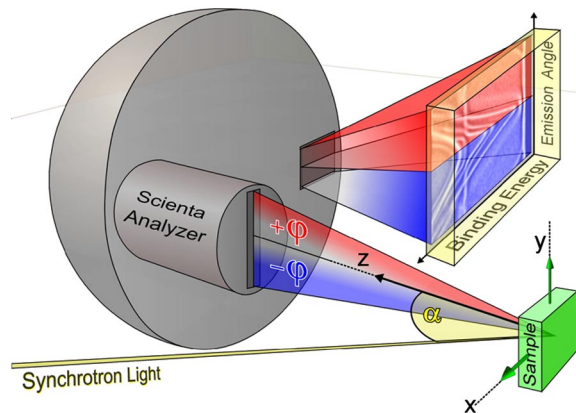


FIG. 1 (color online). Experimental geometry.

cross the $\bar{\Gamma}$ point at a binding energy of 0.1 eV [band (1)] and at E_F [band (2)], respectively. Band (1) follows parabolic behavior with steep slopes, while band (2) is rather flat except at $\bar{\Gamma}$, where it looks to be pushed upward by the arrowhead of the band (1) signal. Two additional PE features approach but do not pass the center of the BZ. One of them [band (3)] reveals steep parabolic dispersion “dressing” on both sides of band (1). Another one [band (4)] is pinned at E_F in the energy region of the expected Kondo resonance. The latter disappears close to the $\bar{\Gamma}$ point as it would be shifted above the Fermi energy.

The described PE signals are compared with bands calculated for a slab consisting of three Si-Rh-Si trilayers with two Yb layers in between. Thus, the surface of the slab is terminated by Si atoms and Yb ions are sitting in the “bulk”. LDA calculations with the Perdew-Wang parametrization for the exchange-correlation potential were performed using the linear muffin-tin orbital method [9,13]. Yb $4f$ electrons were treated as semicore states.

All the experimental bands around $\bar{\Gamma}$ are accurately reproduced by the calculations [Fig. 2(b)]. Particularly bands (1) and (3) are clearly seen in the theoretical data. The experimental observation that the dressing signal [band (3)] is not seen around the center of the BZ is explained by its downward dispersion in the close vicinity of $\bar{\Gamma}$, where it almost merges the signal originating in band (1). The sudden electronlike dispersion of band (3) at $\bar{\Gamma}$ is explained by its interaction with the unoccupied states touching E_F in the center of the BZ.

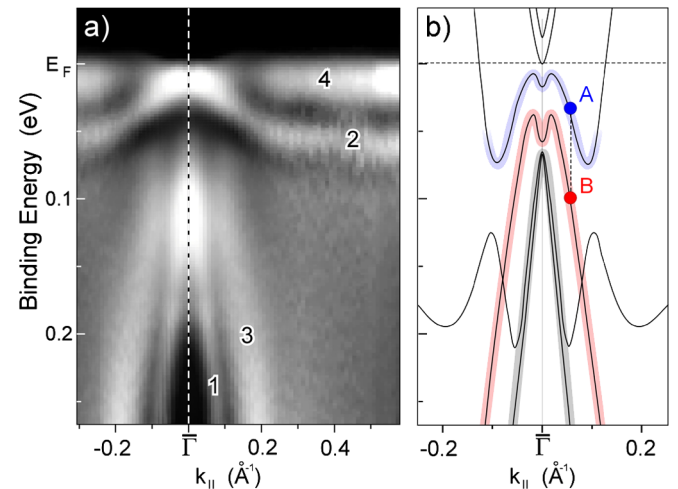


FIG. 2 (color online). (a) PE data taken with $h\nu = 55$ eV along $\bar{\Gamma} - \bar{X}$ (0.78 \AA^{-1}). Light areas correspond to high PE intensity. (b) Results of slab calculations (solid lines). Thick stripes are a guide to the eye to emphasize the electronic structure traced in the experiment. Note, rescaling of the k_{\parallel} axis is necessary for quantitative comparison with the experiment that is caused by the neglect of the $4f$ states at E_F in the calculations. Points **A** and **B** mark electronic states used for the CDAD calculations.

A counterpart of band (2) is also found in the calculations. For $|\mathbf{k}_{\parallel}| > 0.1\text{--}0.2 \text{ \AA}^{-1}$, its dispersion deviates, however, from the experiment where instead of the predicted Fermi-level crossing a dramatic flattening is observed leading to a dispersion almost parallel to E_F for $|\mathbf{k}_{\parallel}| > 0.2 \text{ \AA}^{-1}$. This behavior is obviously caused by interaction with $4f$ states that for a HF system are expected at E_F but are not reproduced by the single-particle calculations where the correlated Yb $4f$ are not taken in the basis set of the VB wave functions. A respective flattening of band (2) around the $\bar{\Gamma}$ point is obviously inhibited by its interaction with a large number of other bands in this region of \mathbf{k} space.

Correspondingly, the signal in the energy region of the expected Kondo contribution for $|\mathbf{k}_{\parallel}| > 0.2 \text{ \AA}^{-1}$ [band (4)] is not predicted by the theory. Its $4f$ origin is concluded from our measurements at $h\nu = 110 \text{ eV}$ (Fig. 3). Essentially only one peak at E_F is visible that decreases in intensity around $\bar{\Gamma}$ in accordance with the Fermi-level crossing of band (4) observed in Fig. 2(a). From the finite intensity of the Fermi-energy peak at $\bar{\Gamma}$ one may conclude, however, that band (2) which approaches E_F in the center of the BZ reveals there considerable $4f$ admixtures. The interaction of this band with the $4f$ states in the region of the Kondo resonance is only possible if in both cases wave functions have similar symmetry properties. The latter will be shown in the following by means of CDAD measurements.

Circular dichroism in angular distribution of photoelectrons has been predicted [14] and verified in PE from not necessarily chiral, but aligned and spatially fixed molecules [11,15] and nonferromagnetic solids [11,16]. The effect requires a “natural” chirality of the sample or at least a handedness of the PE experiment that is present if the direction of photon impact, measured photoelectron momentum, and surface normal are noncoplanar (Fig. 1).

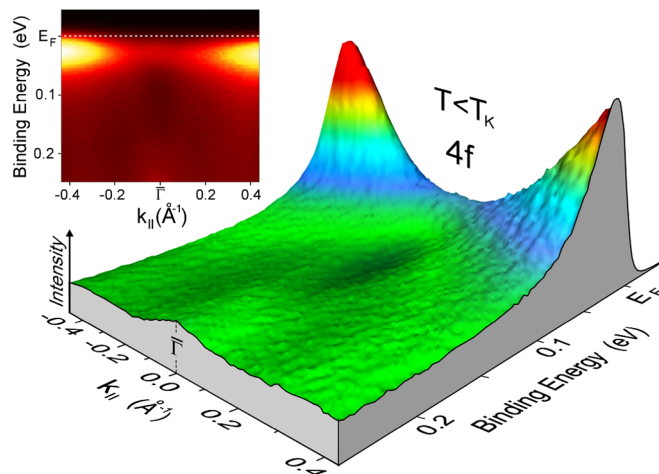


FIG. 3 (color online). PE plot taken at $h\nu = 110 \text{ eV}$. Inset depicts a top view graph of the same data.

Caused by the selected experimental geometry, matrix elements for excitation of a photoelectron from, e.g., even-symmetry states, are affected by possible admixture of odd-symmetry wave functions and *vice versa*. Studied with circularly polarized light, this leads to the observed dichroism which differs in sign for positive and negative \mathbf{k} . Since the mirror image of a right-handed photon is a left-handed one, it is obvious that a change of photon handedness leads to the same effect as a reversal of the direction in \mathbf{k} space. It is reasonable to assume that the states, which reveal the same dichroism behavior, are characterized by similar symmetry properties.

Figure 4 depicts PE data taken with (a) I_+ and (b) I_- polarization. All spectral features are subject to dichroism. The most important observation, however, is that the $4f$ -derived band (4) and the valence band (2) reveal likewise behavior: they are similarly enhanced on the right and left sides of $\bar{\Gamma}$ upon excitation with left and right circularly polarized radiation, respectively. To emphasize the CDAD, an intensity difference plot ($I_+ - I_-$) is shown in Fig. 4(c). As expected from a purely geometric origin of the phenomenon, no dichroism is observed at $\bar{\Gamma}$.

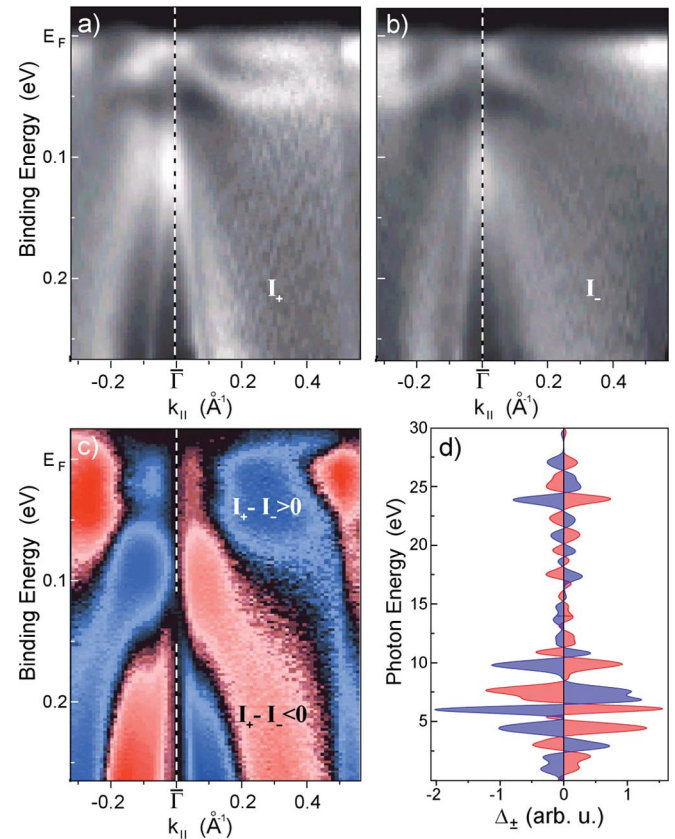


FIG. 4 (color). PE data taken with (a) I_+ and (b) I_- light polarization, $h\nu = 55 \text{ eV}$. (c) Intensity difference ($I_+ - I_-$). Black areas denote regions devoid of dichroism. (d) CDAD calculated for states **A** (blue) and **B** (red) marked in Fig. 2(b), Ref. [17].

Results of our CDAD calculations for YbRh_2Si_2 [17] are presented in Fig. 4(d) for two states **A** and **B** depicted in Fig. 2(b) that differ in mirror symmetry and reveal opposite CDAD effects for all photon energies considered.

From the fact that both the $4f$ signal in the region of the Kondo resonance and the valence band (2) reveal the same sign of CDAD we conclude similar symmetry properties of these states that are responsible for the hybridization effects observed. Like in the case of the $4f$ -derived surface emissions at higher BE [9], $4f$ dispersion is induced by an approaching VB of the same symmetry. As a further consequence of the interaction, $4f$ character is transferred to the VB. Since the center of gravity of the involved bands is expected to remain almost constant upon hybridization, we suppose that on the unoccupied side of the Fermi energy the originally upward dispersing band is replaced by a similarly dispersing hybrid band that reveals strong $4f$ character close to E_F .

The heavy effective masses of the $4f$ -derived bands can be related to the Kondo temperature. Accurate determination of effective masses of the order of $100\text{--}1000m_0$ [2] from PE measurements is, however, not possible. To resolve individual dispersions in a bunch of correspondingly heavy $4f$ bands, both the energy and angle resolutions should be advanced by at least a factor 10 as compared to values available nowadays in ultrahigh energy resolution PE experiments. Another obstacle relates to the fact that the $4f$ bands are located close to E_F and may disperse in the region of the unoccupied states. For the above reasons we make only a rough estimation of the effective masses of the shallow-lying split-off valence band (2) that runs parallel to the $4f$ signal. While close to the $\bar{\Gamma}$ point the obtained effective mass is only $\sim 6m_0$; for $|\mathbf{k}_{\parallel}| > 0.2 \text{ \AA}^{-1}$ it increases toward $30\text{--}60m_0$.

Although dispersion of the individual $4f$ bands in YbRh_2Si_2 is not accessible, our experiments show that the whole bunch of the $4f$ states moves upward in the center of the BZ reducing there the f contributions in the region of the occupied part of the Kondo resonance. This finding proves the \mathbf{k} -dependent properties of the Kondo behavior. In contrast to SIAM results trapping the Kondo peak in Yb systems below the Fermi energy, our data evidence that the Kondo-related intensity can be shifted above E_F owing to coupling to VBs, in particular, regions of the BZ.

This research was funded by the DFG, No. SFB 463, No. TP B4, and No. TP B16. The experiments were supported by the European Commission, No. RII3-CT-2004-506008.

[1] L. Degiorgi, Rev. Mod. Phys. **71**, 687 (1999); G.R. Stewart, Rev. Mod. Phys. **73**, 797 (2001).

- [2] F. Steglich *et al.*, J. Phys. Condens. Matter **8**, 9909 (1996); H. v. Löhneysen, J. Phys. Condens. Matter **8**, 9689 (1996); P. Gegenwart *et al.*, New J. Phys. **8**, 171 (2006).
- [3] P. W. Anderson, Phys. Rev. **124**, 41 (1961); O. Gunnarsson and K. Schönhammer, Phys. Rev. Lett. **50**, 604 (1983); Phys. Rev. B **28**, 4315 (1983).
- [4] S. R. Julian *et al.*, Physica (Amsterdam) **199–200B**, 63 (1994).
- [5] A. B. Andrews *et al.*, Phys. Rev. B **53**, 3317 (1996); H. Kumigashira *et al.*, Phys. Rev. B **55**, R3355 (1997); A. J. Arko *et al.*, Phys. Rev. B **56**, R7041 (1997); M. Garnier *et al.*, Phys. Rev. B **56**, R11399 (1997); J. Boysen *et al.*, J. Alloys Compd. **275–277**, 493 (1998).
- [6] A. B. Andrews *et al.*, Phys. Rev. B **51**, 3277 (1995).
- [7] S. Danzenbächer *et al.*, Phys. Rev. B **72**, 033104 (2005).
- [8] D. V. Vyalikh *et al.*, Phys. Rev. Lett. **96**, 026404 (2006).
- [9] S. Danzenbächer *et al.*, Phys. Rev. Lett. **96**, 106402 (2006); Phys. Rev. B **75**, 045109 (2007); S. L. Molodtsov *et al.*, J. Magn. Magn. Mater. **310**, 443 (2007).
- [10] O. Trovarelli *et al.*, Phys. Rev. Lett. **85**, 626 (2000); J. Custers *et al.*, Nature (London) **424**, 524 (2003); J. Sichelschmidt *et al.*, Phys. Rev. Lett. **91**, 156401 (2003).
- [11] G. Schönhense, Phys. Scr. **T31**, 255 (1990).
- [12] J. W. Cooper, Phys. Rev. **128**, 681 (1962).
- [13] V. Antonov, B. Harmon, and A. Yaresko, *Electronic Structure and Magneto-Optical Properties of Solids* (Kluwer Academic Publishers, Dordrecht, 2004); O. K. Andersen, Phys. Rev. B **12**, 3060 (1975).
- [14] B. Ritchie, Phys. Rev. A **12**, 567 (1975); **13**, 1411 (1976); **14**, 359 (1976); N. A. Cherepkov and V. V. Kuznetsov, Z. Phys. D **7**, 271 (1987); R. L. Dubs *et al.*, Phys. Rev. Lett. **54**, 1249 (1985).
- [15] J. R. Appling *et al.*, J. Chem. Phys. **85**, 6803 (1986); C. Westphal *et al.*, Phys. Rev. Lett. **63**, 151 (1989); T. Jahnke *et al.*, Phys. Rev. Lett. **88**, 073002 (2002).
- [16] G. Schönhense *et al.*, Surf. Sci. **251/252**, 132 (1991).
- [17] The matrix-element (M_- and M_+) calculations were performed in the dipole approximation for the slab as described in the text. The effect of breaking the inversion symmetry on the dichroism $\Delta_{\pm} \sim |M_+|^2 - |M_-|^2$ was simulated by adding constant potential shifts V_i of opposite signs to the potential of two Rh ions which transform into each other under inversion. The calculated net dichroism is proportional to V_i and reveals opposite sign for the Bloch functions, which are even or odd with respect to the reflection by the xy plane. Figure 4(d) presents Δ_{\pm} calculated for $V_i = 0.05 \text{ eV}$ (this value is of the order of the surface potential asymmetry for a slab terminated on the one side by Yb, while on the other side by Si atoms) in a wide range of $h\nu$ for states **A** and **B** [Fig. 2(b)]. Δ_{\pm} could be only followed up to $h\nu = 30 \text{ eV}$, since for higher energies the proper description of the final states fails within the used linear method of band-structure calculations. At any $h\nu$ the calculated CDAD reveals different sign for these two states.